Chemical Physics Letters 469 (2009) 135–139

Contents lists available at ScienceDirect

Chemical Physics Letters

journal homepage: www.elsevier.com/locate/cplett

Quantitative structural relationship and theoretical study of electrochemical properties of C_{60}@[SWCN(5,5)-Armchair-C_nH_{20}] complexes

Avat Arman Taherpour *

Chemistry Department, Faculty of Science, Islamic Azad University, P.O. Box 38135-567, Arak, Iran

ARTICLE INFO

Article history:
Received 23 September 2008
In final form 11 December 2008
Available online 24 December 2008

ABSTRACT

Nanoscale structures of carbon display an attractive variation of structural characteristics, and many useful forms have been synthesized and identified. One of these structures is the carbon nanotubes. Carbon nanotubes are either single-wall (SWCNT) or multi-wall; the former attract more attention due to their unique electronic, optical and spectroscopic properties. The electrochemical properties of the fullerene C_{60} have been studied previously. The accommodation of C_{60} inside the SWCNT leads to significant periodic modifications of the electronic states of SWCNT. One of the main recognized structures of nanotubes is the (5,5) single-wall tube (SWCN). A topological index is a mathematical invariant of a chemical graph, which shows a significant correlation with some chemical or physical property. They have been successfully used to construct effective and useful mathematical methods for finding good relationships between structural data and the properties of these materials. To establish a good structural relationship between the structure of molecules C_{60} and [SWCN(5,5)-Armchair-C_nH_{20}] (n = 20–190) **1–18**, the molecular degree of unsaturation (D_U) was used as one of the useful numerical and structural electrochemical properties of unsaturated compounds. In this study, the relationship between this index and electron affinity; the reduction potential (^{Red}E) of [SWCN(5,5)-Armchair-C_nH_{20}] **1–18** and **19–29**; and the free energy of electron transfer (ΔG_{et}) as assessed using the Rehm–Weller equation between **1–18** and fullerene C_{60} as C_{60}@[SWCN(5,5)-Armchair-C_nH_{20}] **30–47** and **48–58** complexes, are presented.

© 2008 Elsevier B.V. All rights reserved.

1. Introduction

Since the discovery of carbon nanotubes in 1991, SWNTs and MWNTs have been generated that display exceptionally strong and stable mechanical properties along the nanotube's axis and flexible characteristics along the normal to the tube's axis [1–4]. Researchers have tried to exploit nanotube's strength in reinforcing fibers in nanotube-polymer composite materials [5]. Studies of the electronic properties of these materials such as the ionization potential, electron affinity, chemical hardness, and relative energetic stability have produced highly effective results in applications in different areas of science [5,6].

Nanotubes of type (n,n) are called *armchair nanotubes* because of their 'W' shape perpendicular to the tube axis. They are symmetric along the tube axis, with a short unit cell (0.25 nm or 2.5 Å) that can be repeated along the entire section of a long nanotube. All remaining nanotubes are called *chiral nanotubes* and have longer unit cell sizes along the tube axis [6–8]. The simplest type of nanotube is a cylindrical structure that, conceptually, could be formed by folding and gluing one pair of opposite sides of a rectangular graphite sheet [1–17]. If both ends are capped, it will have at least two pentagons and be a type of fullerene. Nanotubes are large, linear fullerenes with aspect ratios as large as 103–105 [7]. The walls of such a tube could have various sizes of polygons [17a–c]. Although many nano-scale fullerene materials occur regularly in applications, controlled production of many fullerenes and nanotubes with well-defined characteristics has not occurred [1–16]. Because of the nanotubes properties, such as the fact that they are hollow, tubular, caged molecules, they can act as lightweight, large surface-area packing material for gas storage and hydrocarbon fuel storage devices, as well as nanoscale applications for molecular drug delivery and casting structures for making nanowires and nanocapsulates. Exceptionally strong nanotubes can be used to make lightweight structural materials. Nanotubes as '*capsulates*' can help to store and carry hydrogen and other hydrocarbon-based fuel in engines or aboard spacecraft. These important groups of carbon allotropes can be easily closed on both sides. Single-wall carbon nanotubes (SWNTs) are among the most interesting new carbon allotropes discovered in many years [6,7].

Carbon nanotubes possess many special properties, such as an open mesoporous structure, high electrical conductivity and chemical stability, as well as extremely high mechanical strength and modulus [8–13]. These properties, which not only help in the

---

* Sabbatical Address: Unusual Molecules and Reactive Intermediates Group, School of Molecular and Microbial Science, Chemistry Building, The University of Queensland, Brisbane-Qld 4072, Australia. Fax: +98 8614130649.
E-mail address: avat_1@Yahoo.co.uk.

0009-2614/$ - see front matter © 2008 Elsevier B.V. All rights reserved.
doi:10.1016/j.cplett.2008.12.039

transportation of ions, but also facilitate the charging of the double layer, will confer advantageous attributes to the developments of electrochemical capacitors [14]. Single-walled carbon nanotubes (SWNTs) have been recognized as a potential electrode material for electrochemical capacitors [15,16].

One of the main recognized structures of nanotubes is the (5,5) tube. In the (5,5) tube, the structure can be built up by successively adjoining sections of 10C atoms. In the infinite tube, the periodic unit cell is two such sections consisting of 20C atoms [6].

The electronic structures and electrical properties of single-wall nanotubes can be simulated from those of a layer of graphite (grapheme sheet) [9–16].

In Fig. 1 the (5,5) *Armchair* form of nanotubes is shown. Fig. 1a shows the expanded form or graphite shapes for the single-wall nanotubes. In experiments, the nanotubes may contain no hydrogens (there is no hydrogen in the electric-arc technique) and the nanotubes can be easily closed at both ends.

The electronic structures of tubular aromatic molecules derived from the metallic (5,5) armchair SWCN for $C_{20}H_{20}$ up to $C_{210}H_{20}$ (see Fig. 1) were reported by Zhou et al. [6]. That report considered how the electronic structures of short molecular sections of the (5,5) tube relate to, differ from, and asymptotically approach the infinite metallic tube [6]. Some of the structural and electronic properties were investigated, such as the ionization potential, electron affinity, Fermi energy (E_f), chemical hardness, and relative energetic stability, all of which show the length periodicity seen in the HOMO–LUMO gap, in contrast to the optical 'charge transfer' transition and the static axial polarizability [6]. These (5,5) nanotubes have two types of symmetry. For nanotubes with odd identification numbers **(1–17)**, the point group is D_{5d}, and for nanotubes with even identification numbers **(2–18)**, the point group is D_{5h}. In that study, static and time-dependent DFT (TD-DFT) were used to independently optimize the structure for neutrals, cations and anions. The hybrid non-local B3LYP functional was utilized [6].

After the discovery of C_{60} peapods by Luzzi et al. [18,19a,19b], the aligned structure of encapsulated molecules due to the molecule–molecule and/or molecule-SWNT interactions has been studied as a new type of hybrid material [19b]. Zhang et al. [19d] reported evidence for the latter interaction by a measurement of the thermal stability of C_{60} peapods [19a–c].

Infinite length SWNTs are π-bonded aromatic structures that can be either semiconducting or metallic, depending upon the diameter and helical angle of SWNTs. In a pioneering 1992 DFT calculation, Mintmire, Dunlap and White predicted that the infinite length (5,5) armchair SWNT (6.70 Å diameter) would be metallic with a very low transition temperature separating the uniform (high temperature) structure from the Peierls bond alternating (low temperature) structure [15]. This specific SWNT is the elongated tube of the C_{60}, C_{70}, etc., molecular family [6].

The electrochemical properties of the fullerene C_{60} have been studied since the early 1990s, when these materials became available in macroscopic quantities (for a review see [20b]) [20a,20b]. In 1990, Haufler et al. [21] have shown that C_{60} is electrochemically reducible in the CH_2Cl_2 medium to C_{60}^{-} and C_{60}^{2-}. In 1992, Echegoyen et al. [22] have cathodically reduced both C_{60} in six reversible one-electron steps for −0.97 vs. Fc/Fc^+ (Fc = ferrocene). This fact, along with the absence of anodic electrochemistry of fullerenes, matches the electronic structure of fullerenes: the LUMO of C_{60} can accept up to six electrons to form C_{60}^{6-}, but the position of the HOMO does not allow for hole-doping under the usual electrochemical conditions. In 1991, Bard et al. [23] first reported on irreversible electrochemical and structural reorganization of solid fullerenes in acetonitrile medium. Dunsch et al. [24] have upgraded the experimental conditions by investigating highly organized C_{60} films on HOPG in aqueous medium. The reduction of such films manifested itself by re-structuring into conductive nanoclusters of $\sim 10^2$ nm in diameter [24,25].

Fullerene peapods are supramolecular complexes, which are formed via filling of SWCNT by fullerenes from the vapor phase [19,20a]. Most reports are related to C_{60}@SWCNT and C_{70}@SWCNT [20,26].

The diameter sizes of C_{60} and [SWCN(5,5)-Armchair-C_nH_{20}] **1–18** were reported to be 6.70 and 6.94 Å, respectively [27]. With these diameters, it is not possible to encapsulate C_{60} inside the [SWCN(5,5)-Armchair-C_nH_{20}] in the structure of C_{60}@[SWCN(5,5)-Armchair-C_nH_{20}] (see the imaginary scheme in Fig. 1).

Graph theory has been found to be a useful tool in assessing the *QSAR* (Quantitative Structure Activity Relationship) and *QSPR* (Quantitative Structure Property Relationship) [28–33]. Numerous studies in the above areas have also used what are called topological indices (TI) [34–37]. It is important to use effective mathematical methods to make good correlations between several data properties of chemicals. One of the useful numerical and structural values in unsaturated compounds like nanotubes is the degree of unsaturation (D_U). This quantity is a useful index for determining the number of cyclic structures and/or π-bonds in a molecule [18a,27,38].

In this study of the structural properties of π-bonds, was attempted to describe a relationship between the D_U index and electron affinity, reduction potential (${}^{Red}E_1$) of [SWCN(5,5)-Armchair-C_nH_{20}] **1–18** (and extension the results to **19–29)** as well as the free energy of electron transfer (ΔG_{et}) between **1–18** and fullerene C_{60} as C_{60}@[SWCN(5,5)-Armchair-C_nH_{20}] **30–47** (and extension the results to **48–58)** complexes.

2. Graphs and mathematical method

The degree of unsaturation (D_U), as a structural index for compounds **(1–18)** with unsaturated hydrocarbonic structure, was determined in these stages: [18a,27,38]

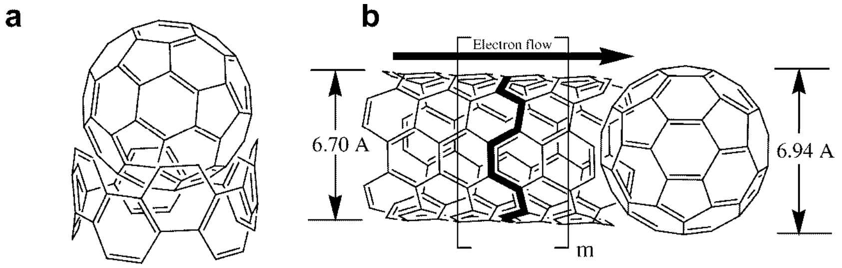

C_{60}@[SWNT(5,5)-Armchair-$C_{20}H_{20}$]

C_{60}@[SWNT(5,5)-Armchair-C_nH_{20}]
n=20-190 **(30-47)** and n=200-300 **(48-58)**

Fig. 1. (a) The imaginary structure of C_{60}@[SWCN(5,5)-Armchair-$C_{20}H_{20}$] and (b) the forms related to the C_{60}@[SWCN(5,5)-Armchair-C_nH_{20}] of (5,5) armchair nanotubes (**30–47** and **48–58**).

(1) Recognition of skeletal structure of compounds **1–18**.
(2) Counting the carbon and hydrogen atoms, and writing the molecular formulae of compounds such as **1–18**. The numbers of hydrogen atoms in compounds are denoted by the 'H_α' symbol.
(3) Transcribing the molecular formula of an *Alkane* according to the number of carbons that were counted in stage-2. The numbers of hydrogen atoms in the molecular formulae are shown with a 'H_β' symbol.
(4) Calculating the 'degree of unsaturation', by comparing the number of H-atoms between stages – 3 and 4. See Eq. (1).

$$D_U = (H_\beta - H_\alpha)/2 \tag{1}$$

The results after some simple mathematical operations are shown in Table 1 for (5,5) nanotubes **1–18**.

All graphing operations were performed using the MICROSOFT OFFICE EXCEL-2003 program. The summation of the degree of unsaturation (D_U) seems a useful numerical and structural value for the empty fullerenes. For modeling, both linear (MLR: Multiple Linear Regressions) and nonlinear (ANN: Artificial Neural Network) models were examined in this study. Some of the other indices were examined and the best results and equations for extending the physicochemical and electrochemical data were chosen.

The Rehm–Weller equation estimates the free energy change between a donor (D) and an acceptor (A) to be:

$$\Delta G^\circ = \mathrm{e}[E^\circ_D - E^\circ_A] - \Delta E^* + \omega_1 \tag{2}$$

where 'e' is the unit electrical charge, E_D and E°_D are the reduction potentials of the electron donor and acceptor, respectively, ΔE^* is the energy of the singlet or triplet excited state, and ω_1 is the work required to bring the donor and acceptor to within the ET distance. The work term in this expression can be considered to be '0' in as much as there exists an electrostatic complex before the electron transfer [39].

3. Discussion

The energy (A_X) is released upon attachment of an electron to an atom or a molecule (X) resulting in the formation of the negative ion X^-, i.e. $X + e^- \rightarrow X^- + A_X$. As in the case of *ionization potential*, one can define an *adiabatic electron affinity* and a *vertical electron affinity*. The adiabatic A_X is equal to the difference between the total energies of a neutral system (X) and the corresponding anion (X^-). The vertical A_X is equal to the difference between the total energies of X and the anion X^- in the equilibrium geometry of X [40]. The free energy of this reaction [$\Delta E_s(A \rightarrow A^-)$] corresponds to the absolute redox energy for the above process. The free energy of an electron (e^-) at rest in the gas phase is set to zero [41,42]. It is possible to calculate the redox energy of reaction ($X + e^- \rightarrow X^- + A_X$) using the thermodynamic equation (see Eq. (3)). In this equation, $\Delta G_s(A)$ and $\Delta G_s(A^-)$ are the solvation energies of molecule A and its anion A^-, respectively, and $\Delta E_g(A \rightarrow A^-)$ is the energy difference between molecule A and its anion (which is defined as the redox energy in the gas phase). On the basis of this thermodynamic cycle, one can obtain $\Delta E_s(A \rightarrow A^-)$, the absolute redox energy, by [41,42]:

$$\Delta E_S(A \rightarrow A^-) = \Delta E_g(A \rightarrow A^-) + \Delta G_S(A) - \Delta G_S(A^-) \tag{3}$$

Table 1
The values of the relative structural coefficients of [SWCN(5,5)-Armchair-C_nH_{20}] (n = 20–190) **1–18** and C_{60}@[SWCN(5,5)-Armchair-C_nH_{20}] **30–47**.[a] Values for all species were calculated and reported at the 6-31G* level. (See Ref. [1]).

No.	Molecular formula	Point group	D_u	Adiabatic electron affinity E_{aa} (eV)	${}^{Red}E$ (V)	No.	ΔG_{et} (kcal mol^{-1})[a] C_{60}@[SWCN(5,5)-Armchair-C_nH_{20}] **30–47**
1	$C_{20}H_{20}$	D_{5d}	11	0.34	−0.34	30	35.05
2	$C_{30}H_{20}$	D_{5h}	21	0.89	−0.89	31	47.73
3	$C_{40}H_{20}$	D_{5d}	31	0.67	−0.67	32	42.66
4	$C_{50}H_{20}$	D_{5h}	41	1.14	−1.14	33	53.50
5	$C_{60}H_{20}$	D_{5d}	51	1.56	−1.56	34	63.18
6	$C_{70}H_{20}$	D_{5h}	61	1.34	−1.34	35	58.11
7	$C_{80}H_{20}$	D_{5d}	71	1.61	−1.61	36	64.34
8	$C_{90}H_{20}$	D_{5h}	81	1.98	−1.98	37	72.87
9	$C_{100}H_{20}$	D_{5d}	91	1.71	−1.71	38	66.64
10	$C_{110}H_{20}$	D_{5h}	101	1.91	−1.91	39	71.25
11	$C_{120}H_{20}$	D_{5d}	111	2.24	−2.24	40	78.86
12	$C_{130}H_{20}$	D_{5h}	121	2.06	−2.06	41	74.71
13	$C_{140}H_{20}$	D_{5d}	131	2.13	−2.13	42	76.33
14	$C_{150}H_{20}$	D_{5h}	141	2.43	−2.43	43	83.25
15	$C_{160}H_{20}$	D_{5d}	151	2.35	−2.35	44	81.40
16	$C_{170}H_{20}$	D_{5h}	161	2.23	−2.23	45	78.63
17	$C_{180}H_{20}$	D_{5d}	171	2.53	−2.53	46	85.55
18	$C_{190}H_{20}$	D_{5h}	181	2.45	−2.45	47	83.71

[a] The compounds C_{60}@[SWCN(5,5)-Armchair-C_nH_{20}] **30–47** were not synthesized or reported. The data of ΔG_{et} (kcal mol^{-1}) for compounds **30–47** were calculated by the Rehm–Weller equation and the complexes were not reported.

Thus, by calculating the gas phase energies and solvation energies of molecule A and its anion A^-, one can derive the absolute redox potential (scaled) of molecule A in solution. A scaling coefficient that translates electron affinity to standard redox potentials can be thus extracted [42].

With respect to the interesting results of Ref. [1]: The static and time-dependent DFT (TD-DFT) and independently optimized structure were used to calculate the physicochemical and electronic structure of tubular aromatic molecules derived from the metallic (5,5) armchair single-wall carbon nanotubes. The hybrid non-local B3LYP functional was employed [6,43–45].

In the most elementary cluster model, the ionization potential of a small metal or semiconductor particle differs from the negative of the bulk Fermi energy ($-E_f$) by a classical charging energy plus a quantum size effect term [6,46,47]. The charging energy by itself at high particle dielectric constant gives a correction to the ionization potential I_p, $I_p = -E_f + e^2/2R$, and to the electron affinity E_a) $E_a = -E_f - e^2/2R$. Here, R is the cluster radius. The ionization potential is larger than the electron affinity, as is the normal situation for molecules. For very small clusters, the electron affinity may even become negative [6].

It is possible to calculate the reduction potential (${}^{Red}E$) of **1–18** using the Gibbs equation ($\Delta G = -n\mathrm{FE}$) and the definition of adiabatic electron affinity. In this equation, ΔG is equal to the adiabatic electron affinity (the free energy of electron transfer, ΔG_{et} in J mol^{-1}, 1 eV = 96471 J mol^{-1}, F = 96495 coulomb and n = 1). For example, the reduction potentials (${}^{Red}E$) of $C_{20}H_{20}$ and $C_{30}H_{20}$ are equal to −0.34 and −0.89 V. The reduction potentials (${}^{Red}E$) of [SWCN(5,5)-Armchair-C_nH_{20}] (n = 20–190) **1–18** have been calculated and are presented in Table 1. As a rapid result the amount of ${}^{Red}E$ (in V) = $-E_{aa}$ (in eV). E_{aa} is the adiabatic electron affinity.

It is recognized that buckminsterfullerene C_{60} is a highly electronegative molecule [48a–e,49]. As an electron acceptor, the first oxidation potential ${}^{ox}E_1$ of C_{60} was reported to be +1.21 V [46]. The ${}^{ox}E_1$ value for C_{60} was obtained in the irreversible condition and by DPV (Differential Pulse Voltammogram), pulse amplitude, 50 mV, pulse width, 50 ms, pulse period, 200 ms and scan rate of 20 mV/s. The value of the diameter of C_{60} was reported to be 6.94 Å.

The values of the relative structural coefficients of the (5,5) armchair SWCN for $C_{20}H_{20}$ up to $C_{190}H_{20}$ ([SWCN(5,5)-Armchair-C_nH_{20}], **1–18**), the degree of unsaturation (D_U), the adiabatic electron affinity (E_{aa} in eV) and the reduction potentials (${}^{Red}E$ in V) of **1–18** are shown in Table 1. The values shown in Table 1 demonstrate that the degree of unsaturation (D_U) increases with the molecular size of compounds **(1–18)**. Table 1 reveals that the distances of D_U between compounds **1** to **18** are 10 units. The numbers shown in Table 1 for **1–18** (and extended in Table 1 for compounds **19–29**) have some mathematical structures. The absolute values of E_{aa} or ${}^{Red}E$ increase with increasing D_U in **1–18**. From $C_{20}H_{20}$ up to $C_{190}H_{20}$, the point groups alternated between D_{5d} and D_{5h}.

Table 1 also shows the values of the free energy of electron transfer (ΔG_{et}) by the Rehm–Weller equation between C_{60} and [SWCN(5,5)-Armchair-C_nH_{20}], **1–18** in the structures C_{60}@[SWCN(5,5)-Armchair-C_nH_{20}] **30–47** (n = 20–190).

The results of the reduction potentials (${}^{Red}E$ in V) were extended for $C_{210}H_{20}$ up to $C_{300}H_{20}$ ([SWCN(5,5)-Armchair-C_nH_{20}], **19–29**). The calculated results for ${}^{Red}E$, as well as the free energy of electron transfer (ΔG_{et}) according to the Rehm–Weller equation between C_{60} and [SWCN(5,5)-Armchair-C_nH_{20}], **19–29** in the structures C_{60}@[SWCN(5,5)-Armchair-C_nH_{20}] **48–58** (n = 210–300) are presented in Table 2.

Fig. 2 shows the curve of the relationship between the values of the 'D_U' versus the adiabatic electron affinity (E_{aa} in eV) of [SWCN(5,5)-Armchair-C_nH_{20}] (n = 20–190) **1–18** as presented in Table 1. Eq. (4) applies to Fig. 2 and shows the *Nieperian* logarithmic behavior of the relationship. Using this equation, it is possible to achieve a good approximation for extending the adiabatic electron affinity (E_{aa} in eV) for the other [SWCN(5,5)-Armchair-C_nH_{20}] (n = 200–300) **19–29**. The R-squared value (R^2) for this graph is equal to 0.9374.

$$E_{aa} = 0.8062\ \mathrm{Ln}(D_U) - 1.748 \tag{4}$$

The predicted values of E_{aa} for [SWCN(5,5)-Armchair-C_nH_{20}] (n = 200–300) **19–29** were calculated using Eq. (4) (see Table 2).

Eq. (5) shows the relationship between the values of the molecular degree of unsaturation 'D_U' versus the reduction potential (${}^{Red}E$ in V) of [SWCN(5,5)-Armchair-C_nH_{20}] (n = 20–190) **1–18**. Eq. (5) similar to the Eq. (4) shows the *Nieperian* logarithmic behavior of the relationship. The R-squared value (R^2) for this graph is equal to 0.9374.

$${}^{Red}E = -0.8062\ \mathrm{Ln}(D_U) + 1.748 \tag{5}$$

Using this equation, it is possible to achieve a good approximation for extending the determination of the reduction potential (${}^{Red}E$) for the other [SWCN(5,5)-Armchair-C_nH_{20}] (n = 200–300) **19–29**.

The relationship between the values of the 'D_U' of [SWCN(5,5)-Armchair-C_nH_{20}] (n = 20–190) **1–18** versus the free energy of electron transfer (ΔG_{et} in kcal mol^{-1}) of C_{60}@[SWCN(5,5)-Armchair-C_nH_{20}] **30–47** is shown in Eq. (6). The Eq. (6) also exhibits *Nieperian* logarithmic behavior. The R-squared value (R^2) for this graph is equal to 0.9374.

$$\Delta G_{et} = 18.592\ \mathrm{Ln}(D_U) - 13.101 \tag{6}$$

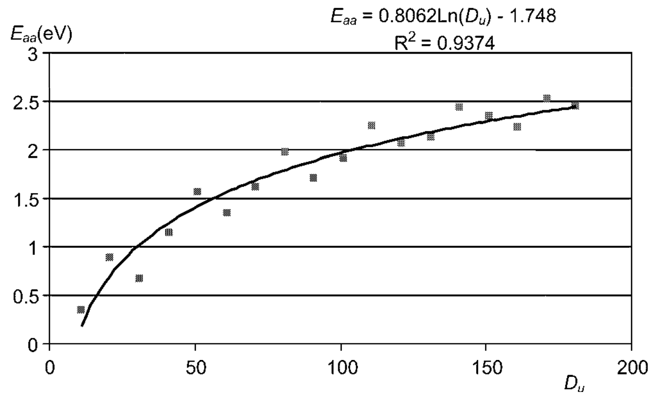

Fig. 2. The relationship between the values of 'D_U' and the adiabatic electron affinity (E_{aa} in eV) of [SWCN(5,5)-Armchair-C_nH_{20}] (n = 20–190) **1–18**.

Using this equation, it is possible to extend the calculation of the free energy of electron transfer (ΔG_{et} in kcal mol^{-1}) for some of the other supramolecular structures of C_{60}@[SWCN(5,5)-Armchair-C_nH_{20}] **30–47**.

There are very good linear relationships between the values of the adiabatic electron affinity (E_{aa} in eV) and the values of the reduction potential (${}^{Red}E$ in V) of [SWCN(5,5)-Armchair-C_nH_{20}] (n = 20–190) **1–18** versus the free energy of electron transfer (ΔG_{et} in kcal mol^{-1}) of C_{60}@[SWCN(5,5)-Armchair-C_nH_{20}] **30–47**, respectively. Eqs. (7) and (8) are used to the correlations, respectively, giving the R-squared value (R^2) for these two relationships of 1.00.

$$\Delta G_{et} = 23.06(E_{aa}) + 27.209 \tag{7}$$

$$\Delta G_{et} = -23.06({}^{Red}E) + 27.209 \tag{8}$$

In light of the good linear correlations between ΔG_{et} and E_{aa} and ${}^{Red}E$ of **1–18** and **30–47**, respectively it is possible to use the values of E_{aa} and ${}^{Red}E$ to calculate the free energy of electron transfer (ΔG_{et} in kcal mol^{-1}) of C_{60}@[SWCN(5,5)-Armchair-C_nH_{20}] (n = 20–300) **30–47** & **48–58**. The electron affinity and the reduction potential are in fact the same magnitude with the sign reversed, whereas the free energy of electron transfer is calculated with the Rehm–Weller equation, which can be straightforwardly proven to be linearly depending on the electron affinity of compounds studied here. In Table 2 the values of the free energy of electron transfer obtained for compounds **48–58** from Eqs. (7) and (8) and those obtained with the Rehm–Weller equation (values in parenthesis) are compared. Obviously these numbers are equal since those calculated with the Rehm–Weller equation were calculated using electron affinities obtained from Eq. (4), which is in fact equivalent to Eq. (6).

Table 2
The values of the relative structural coefficients of [SWCN(5,5)-Armchair-C_nH_{20}] (n = 20–190) **19–29** and C_{60}@[SWCN(5,5)-Armchair-C_nH_{20}] **48–58**.

No.	Molecular formula	Point group	D_u	Adiabatic electron affinity E_{aa} (eV)	${}^{Red}E$ (V)	No.	ΔG_{et} (kcal mol^{-1})[a] C_{60}@[SWCN(5,5)-Armchair-C_nH_{20}] **48–58**	
							Eq. (7) &/or (8)	Rehm–Weller equation
19	$C_{200}H_{20}$	D_{5d}	191	2.49	−2.49	48	84.63	(84.63)
20	$C_{210}H_{20}$	D_{5h}	201	2.53	−2.53	49	85.55	(85.55)
21	$C_{220}H_{20}$	D_{5d}	211	2.57	−2.57	50	86.47	(86.47)
22	$C_{230}H_{20}$	D_{5h}	221	2.60	−2.60	51	87.16	(87.16)
23	$C_{240}H_{20}$	D_{5d}	231	2.64	−2.64	52	88.09	(88.09)
24	$C_{250}H_{20}$	D_{5h}	241	2.67	−2.67	53	88.78	(88.78)
25	$C_{260}H_{20}$	D_{5d}	251	2.71	−2.71	54	89.70	(89.70)
26	$C_{270}H_{20}$	D_{5h}	261	2.74	−2.74	55	90.39	(90.39)
27	$C_{280}H_{20}$	D_{5d}	271	2.77	−2.77	56	91.08	(91.08)
28	$C_{290}H_{20}$	D_{5h}	281	2.80	−2.80	57	91.78	(91.78)
29	$C_{300}H_{20}$	D_{5d}	291	2.83	−2.83	58	92.47	(92.47)

[a] The species data were calculated using Eqs. (1), (2), (4)–(8). The data in parenthesis of ΔG_{et} (kcal mol^{-1}) for compounds **48–58** were calculated using the Rehm–Weller equation, and the complexes were not synthesized and reported.

The values of D_U, E_{aa}, ${}^{Red}E$ and ΔG_{et} of [SWCN(5,5)-Armchair-C_nH_{20}] ($n = 200$–300) **19–29** and their complexes with C_{60} (C_{60}@[SWCN(5,5)-Armchair-C_nH_{20}] ($n = 200$–300) **48–58**) are shown in Table 2. In Fig. 2 the periodicity of the points plotted which appear to be 3, is quite common among benzenoids. By using Eq. (1) (for D_U), (2) (Rehm–Weller equation) and (4)–(7) (or Eq. (8)) the values of D_U, E_{aa}, ${}^{Red}E$ and ΔG_{et} were calculated for **19–29** and **48–58**. The values of the degree of unsaturation (D_U) show a good relationship with the values of the adiabatic electron affinity (E_{aa} in eV), the values of the reduction potential (${}^{Red}E$ in V) of [SWCN(5,5)-Armchair-C_nH_{20}] ($n = 20$–190) **1–18** & **19–29** and the free energy of electron transfer (ΔG_{et} in kcal mol^{-1}) in the C_{60}@[SWCN(5,5)-Armchair-C_nH_{20}] ($n = 20$–300) **30–47** & **48–58.** With the above equations, it is possible to calculate the adiabatic electron affinity (E_{aa} in eV), the values of the reduction potential (${}^{Red}E$ in V) in **1–18** & **19–29** and the free energy of electron transfer (ΔG_{et} in kcal mol^{-1}) in the **30–47** & **48–58** with good approximation. The armchair single-wall nanotubes [SWCN(5,5)-Armchair-C_nH_{20}] ($n = 20$–300) **1–18** & **19–29** and their supramolecular complexes with C_{60} i.e. C_{60}@[SWCN(5,5)-Armchair-C_nH_{20}] ($n = 20$–300) **30–47** & **48–58** were neither synthesized nor reported.

4. Conclusion

Nano-scale materials have been applied in many areas of sciences such as computers, microchips, sensors, actuators and machines. Graph theory applications have provided different mathematical methods for finding the relationships between several numerical properties of the materials. In this study, the structural relationships between the degree of unsaturation (D_U) index and the adiabatic electron affinity (E_{aa} in eV), the values of the reduction potential (${}^{Red}E$ in V) of [SWCN(5,5)-Armchair-C_nH_{20}] ($n = 20$–190) **1–18** & **19–29** and the free energy of electron transfer (ΔG_{et} in kcal mol^{-1}) in the C_{60}@[SWCN(5,5)-Armchair-C_nH_{20}] ($n = 20$–300) **30–47** & **48–58** were demonstrated. The values of the degree of unsaturation D_U show strong correlation with the values of E_{aa} and ${}^{Red}E$ in the (5,5) armchair SWCN **1–18** & **19–29** as an important factors in these materials. The value of ΔG_{et} was calculated using the Rehm–Weller equation in C_{60}@[SWCN(5,5)-Armchair-C_nH_{20}] ($n = 20$–300) **30–47**. Using this model and the associated equations, it is possible to calculate in a simple manner and with good approximation the E_{aa}, ${}^{Red}E$ and ΔG_{et} of this family of compounds **19–29** and the complexes with C_{60} **48–58**. The model can be used to study structural properties, the electron affinity, the reduction potential and the free energy of electron transfer properties of these types of nanotubes (5,5), armchair SWCN and their supramolecular structures C_{60}@[SWCN(5,5)-Armchair-C_nH_{20}].

Acknowledgments

The author gratefully acknowledges his colleagues in the Chemistry Department of The University of Queensland-Australia, for their useful suggestions.

References

[1] J.S. Arellano, L.M. Molina, A. Rubio, M.J. Lopez, J.A. Alonso, J. Chem. Phys. 117 (5) (2002) 2281.

[2] D. Srivastava, S. Barnard, in: Proc. IEEE Supercomputing '97, IEEE Computer Soc. Press, Los Alamitos, California, 1997.

[3] B.I. Yakobson, C.J. Brabec, J. Bernholc, Phys. Rev. Lett. 76 (1996) 2511.

[4] D. Srivastava, M. Menon, K. Cho, Phys. Rev. Lett. 83 (1999) 2973.

[5] B.I. Yakobson, P. Avouris, Mechanical Properties of Carbon Nanotubes, Carbon Nanotubes, Springer-Verlag, Berlin, 2001. p. 293.

[6] Z. Zhou, M. Steigerwald, M. Hybertsen, L. Brus, R.A. Friesner, J. Am. Chem. Soc. 126 (11) (2004) 3597 (and the literature cited therein).

[7] D. Srivastava, M. Menon, K. Cho, Comp. Sci. Eng. (2001) 42.

[8] O. Lourie, D.M. Cox, H.D. Wagner, Phys. Rev. Lett. 81 (1998) 1638.

[9] M.S. Dresselhaus, G. Dresselhaus, P.C. Eklund, Science of Fullerenes and Carbon Nanotubes, Academic Press, New York, 1996.

[10] P. Avouris, Acc. Chem. Res. 35 (2002) 1026.

[11] M.S. Dresselhaus, G. Dresselhaus, Ph. Avouris, Carbon Nanotubes: Synthesis, Structure Properties and Applications, Springer-Verlag, Berlin, 2001.

[12] Special issue on carbon nanotubes, Phys. World, 13 (6) (2000).

[13] P.G. Collins, Ph. Avouris, Nanotube. Electron. Sci. Am. 283 (2000) 38.

[14] M.S. Dresselhaus, G. Dresselhaus, R. Saito, Symm. Phys. Rev. B 45 (1992) 6234.

[15] J.W. Mintmire, B.I. Dunlap, C.T. White, Phys. Rev. Lett. 68 (1992) 631.

[16] R. Barnett, E. Demler, E. Kaxiras, Solid State Comm. 135 (2005) 335.

[17] (a) M.V. Diudea, Fulleren. Nanotube Carbon Nanostruct. 10 (2002) 273;
(b) M.V. Diudea, Studia Univ. Babes-Bolyai 48 (2003) 23;
(c) M.V. Diudea, in: M.V. Diudea (Ed.), Nanostructures, Novel Architecture, NOVA, 2005, pp. 111–126.

[18] (a) H. Shen, Mol. Phys. 105 (17–18) (2007) 2405;
(b) A.A. Taherpour, Fulleren. Nanotube Carbon Nanostruct. 17 (2009), in press.

[19] (a) K. Kimura, N. Ikeda, Y. Maruyama, T. Okazaki, H. Shinohara, S. Bandow, S. Iijima, Chem. Phys. Lett. 379 (2003) 340;
(b) B.W. Smith, M. Monthioux, D.E. Luzzi, Nature 396 (1998) 3239;
(c) T. Miyake, S. Saito, Solid State Commun. 125 (2003) 201;
(d) M. Zhang, M. Yudasaka, S. Bandow, S. Iijima, Chem. Phys. Lett. 369 (2003) 680.

[20] (a) L. Kavan, L. Dunsch, H. Kataura, Carbon 42 (2004) 1011;
(b) B.S. Sherigara, W. Kutner, F. D'Souza, Electroanalysis 15 (2003) 753.

[21] R.E. Haufler, J. Conceicao, L.P.F. Chibante, Y. Chai, N.E. Byrne, S. Flanagan, et al., J. Phys. Chem. 94 (1990) 8634.

[22] Q. Xie, E. Perez-Codero, L. Echegoyen, J. Am. Chem. Soc. 114 (1992) 3978.

[23] C. Jehoulet, Y.O. Obeng, Y.T. Kim, F. Zhou, A.J. Bard, J. Am. Chem. Soc. 114 (1992) 4237.

[24] P. Janda, T. Krieg, L. Dunsch, Adv. Mater. 17 (1998) 1434.

[25] A. Touzik, H. Hermann, P. Janda, L. Dunsch, K. Wetzig, Europhys. Lett. 60 (2002) 411.

[26] S. Bandow, M. Takizawa, H. Kato, T. Okazaki, H. Shinohara, S. Iijima, Chem. Phys. Lett. 347 (2001) 23.

[27] (a) A.A. Taherpour, Fulleren. Nanotube Carbon Nanostruct. 16 (2008) 196;
(b) A.A. Taherpour, Fulleren. Nanotube Carbon Nanostruct. 15 (2007) 279.

[28] A.A. Taherpour, F. Shafiei, J. Mol. Struct. Theochem. 726 (2005) 183.

[29] P.J. Hansen, P. Jurs, J. Chem. Edu. 65 (1988) 574. and the literature cited therein.

[30] H. Hosoya, Bull. Chem. Soc. Jpn. 44 (1971) 2332.

[31] M. Randić, Acta Chim. Slov. 45 (1998) 239.

[32] G. Rücker, C. Rücker, J. Chem. Inf. Comput. Sci. 39 (1999) 788.

[33] H. Wiener, J. Am. Chem. Soc. (1947) 17.

[34] Y.P. Du, Y.Z. Liang, B.Y. Li, C.J. Xu, J. Chem. Inf. Comput. Sci. 42 (2002) 1128.

[35] M. Randić, J. Am. Chem. Soc. 97 (1975) 6609.

[36] S.D. Bolboaca, L. Jantschi, Int. J. Mol. Sci. 8 (2007) 335.

[37] Z. Slanina, F. Uhlik, S.L. Lee, E. Osawa, MATCH Commun. Math. Comput. Chem. 44 (2001) 335.

[38] A.A. Taherpour, Aus. J. Ed. Chem. 65 (2005) 37.

[39] D. Rehm, A. Weller, Isr. J. Chem. 8 (1970) 259.

[40] Cite of: International Union of Pure and Applied Chemistry.htm, Pure Appl. Chem. 71 (10) (1999) 1919.

[41] L.Y. Hang, R.A. Friesner, J. Phys. Chem. 99 (1995) 16479.

[42] I.A. Topol et al., Protein Sci. 10 (7) (2001) 1434.

[43] A.D. Becke, J. Chem. Phys. 98 (1993) 5648.

[44] K. Raghavachari, Theor. Chem. Acc. 103 (2000) 361.

[45] (a) J. Muscat, A. Wander, N.M. Harrison, Chem. Phys. Lett. 342 (2001) 397;
(b) J.K. Perry, J. Tahir-Kheli, W.A. Goddard, Phys. Rev. B 65 (2002) 144501;
(c) K.N. Kudin, G.E. Scuseria, R.L. Martin, Phys. Rev. Lett. 89 (2002) 266402.

[46] L.E. Brus, J. Chem. Phys. 79 (1983) 5566.

[47] G. Makov, A. Nitzan, L.E. Brus, J. Chem. Phys. 88 (1988) 5076.

[48] (a) Y. Murata, K. Motoyama, K. Komatsu, Tetrahedron 52 (14) (1996) 5077;
(b) R. Taylor, D.R.M. Walton, Nature 363 (1993) 685;
(c) G.A. Olah, I. Bucsi, R. Aniszfeld, G.K.S. Prakash, Carbon 30 (1992) 1203;
(d) A. Hirsch, The Chemistry of the Fullerenes, Georg Thieme Verlag, Suttgart, 1994;
(e) See also P.D.W. Boyd, P. Bhyrappa, P. Paul, J. Stinchcombe, R.D. Bolskar, Y. Sun, C.A. Reed, J. Am. Chem. Soc. 117 (1995) 2907. and the literature cited therein.

[49] T. Suzuki et al., Tetrahedron 52 (14) (1996) 4973.